Supplement of Atmos. Chem. Phys., 19, 89–113, 2019
https://doi.org/10.5194/acp-19-89-2019-supplement

Atmospheric Chemistry and Physics
Open Access
EGU

Supplement of

New particle formation in the marine atmosphere during seven cruise campaigns

Yujiao Zhu et al.

Correspondence to: Xiaohong Yao (xhyao@ouc.edu.cn)

List of Texts:

S1 Chemical analysis of the nano-MOUDI or MOUDI sample filters.

S2 Calculations of the new particle formation rate (FR), growth rate (GR) and condensation sink (CS).

List of Figures:

Figure S1 Satellite value of NO_2 (GOME-2 observation) during November 2012 (a), May 2014 (b), August 2015 (c) and April 2014 (d).

Figure S2 Comparison of $N_{<30\ nm}$ and D_{pg} during four NPF days in 2012 (A: 14 October, B: 15 October, C: 17 October, D: 18 October).

Figure S3 Seasonal variations in the average particle size distributions over the marginal seas of China.

Figure S4 Relationship of the condensation sink (CS) with the formation rate (FR) and growth rate (GR) over the marine (NWPO and marginal seas) and at the OUC site (the solid markers represent the simultaneous NPF events).

Figure S5 Relationship between the net maximum increase in the nucleation mode particles number concentration (NMINP) and new particle formation rate (FR), maximum geometric median diameter of new particles (D_{pgmax}) and growth rate (GR) in NPF events occurred at the OUC site (the black symbols were treated as outliers and excluded from the correlation analysis).

Figure S6 24-h air mass back trajectories on NPF days from 2012 to 2015 (the red lines represent the ship location, and the blue lines represent the location of OUC).

Figure S7 Height of the air mass back trajectories on 8 and 13 April 2014 over the NWPO.

Figure S8 24-h air mass back trajectory throughout the NPF events and sampling periods (from 7:00 to 24:00 on 8 April 2014 and from 7:00 to 21:00 on 13 April 2014).

List of Tables:

Table S1 Comparison of same NPF events measured by FMPS and SMPS.

S1 Chemical analysis of the nano-MOUDI or MOUDI sample filters.

The collected samples were wrapped with baked aluminum foils (pre-combusted at 450℃ for 6 h in a furnace to eliminate the absorbed organic compounds) and sealed in polyethylene bags, then stored in darkness at -20℃ before chemical analysis. All samples were ultrasonically extracted in deionized water (18.2 MΩ•cm) for 20 min at 0℃. The mass concentrations of sodium (Na^+), ammonium (NH_4^+), potassium (K^+), magnesium (Mg^{2+}), calcium (Ca^{2+}), dimethylammonium (DMA^+), trimethylammonium (TMA^+), chloride (Cl^-), nitrite (NO_2^-), nitrate (NO_3^-), sulfate (SO_4^{2-}), phosphate (PO_4^{3-}), formate (HCO_2^-), acetate ($C_2H_3O_2^-$), oxalate ($C_2O_4^{2-}$) and succinate ($C_4H_4O_4^{2-}$) were determined using Dionex ICS-3000 and Dionex ICS-1100 ion chromatographs equipped with different analytic columns. The QA/QC was detailed in Hu et al. (2015). All results were corrected with field blanks.

S2 Calculations of the new particle formation rate (FR), growth rate (GR) and condensation sink (CS).

The formation rate of new particles (FR), taking consideration of the coagulation and growth losses, was calculated using the method provided by Sihto et al., (2006):

$$\mathrm{FR} = \frac{dN_{dp}}{dt} + CoagS_{dp} \cdot N_{dp} + \frac{GR}{\Delta d_p} \cdot N_{dp} + S_{losses} \quad (1)$$

where d_p is the sizes of nucleation mode particles. For FMPS, it is denoted by 5.6-30 nm particles, while for SMPS, it is denoted by 10-30 nm particles. N_{dp} is the particle number concentration of nucleation mode particles. The coagulation loss for particles ($CoagS_{dp} \cdot N_{dp}$) was the sum of particle-particle inter- and hetero-coagulation rates. The growth loss ($GR/\triangle d_p \cdot N_{dp}$) is due to condensation growth out of the nucleation mode sizes during the calculation period. S_{losses} includes additional losses and is assumed to be zero.

The apparent growth rate (GR) of new particles was calculated by:

$$GR = \frac{\Delta D_{pg}}{\Delta t} \quad (2)$$

where D_{pg} was fitted by the multiple log-normal distribution functions (Whitby, 1978; Zhu et al., 2014), and Δt was the duration for the growth of new particles.

The condensation sink (CS) is the loss rate of condensable vapor molecules onto the pre-existing particles, and calculated as Kulmala et al. (2001, 2005) and Dal Maso et al. (2005):

$$CS = 2\pi D \int D_p \beta_M(D_p) n(D_p) dD_p = 2\pi D \sum_i \beta_{Mi} D_{pi} N_{pi} \quad (3)$$

where D is the diffusion coefficient, β_M is the transitional regime correction factor, D_{pi} is the particle diameter of size class i, and N_{p_i} is the particle number concentration in size class i.

References

Dal Maso, M., Kulmala, M., Riipinen, I., Wagner, R., Hussein, T., Aalto, P. P., and Lehtinen, K. E. J.: Formation and growth of fresh atmospheric aerosols: Eight years of aerosol size distribution data from SMEAR II, Hyytiala, Finland, Boreal Environ. Res. 10, 323-336, 2005.

Hu, Q., Yu, P., Zhu, Y., Li, K., Gao, H., and Yao, X. Concentration, size distribution, and formation of trimethylaminium and dimethylaminium ions in atmospheric particles over marginal seas of China, J. Atmos. Sci., 72, 3487-3498, doi:10.1175/JAS-D-14-0393.1, 2015.

Kulmala, M., Dal Maso, M., Mäkelä, J. M., Pirjola, L., Väkevä, M., Aalto, P., Miikkulainen, P., Hämeri, K., and O'Dowd, C. D.: On the formation, growth and composition of nucleation mode particles, Tellus B, 53, 479-490, doi:10.1034/j.1600-0889.2001.530411.x, 2001.

Kulmala, M., Petäjä, T., Mönkkönen, P., Koponen, I.K., Dal Maso, M., Aalto, P. P., Lehtinen, K. E. J., and Kerminen, V. M.: On the growth of nucleation mode particles: Source rates of condensable vapor in polluted and clean environments. Atmos. Chem. Phys., 5, 409-416, doi:10.5194/acp-5-409-2005, 2005.

Sihto, S.-L., Kulmala, M., Kerminen, V.-M., Dal Maso, M., Petäjä,T., Riipinen, I., Korhonen, H., Arnold, F., Janson, R., Boy, M., Laaksonen, A., and Lehtinen, K. E. J.: Atmospheric sulphuric acid and aerosol formation: implications from atmospheric measurements for nucleation and early growth mechanisms, Atmos. Chem. Phys., 6, 4079–4091, doi:10.5194/acp-6-4079-2006, 2006.

Whitby, K. T.: The physical characteristics of sulfur aerosols, Atmos. Environ., 12, 135-159, doi:10.1016/0004-6981(78)90196-8, 1978.

Zhu, Y., Sabaliauskas, K., Liu, X., Meng, H., Gao, H., Jeong, C. H., Evans, G. J., and Yao, X.: Comparative analysis of new particle formation events in less and severely polluted urban atmosphere, Atmos. Environ., 98, 655-664, doi:10.1016/j.atmosenv.2014.09.043, 2014.

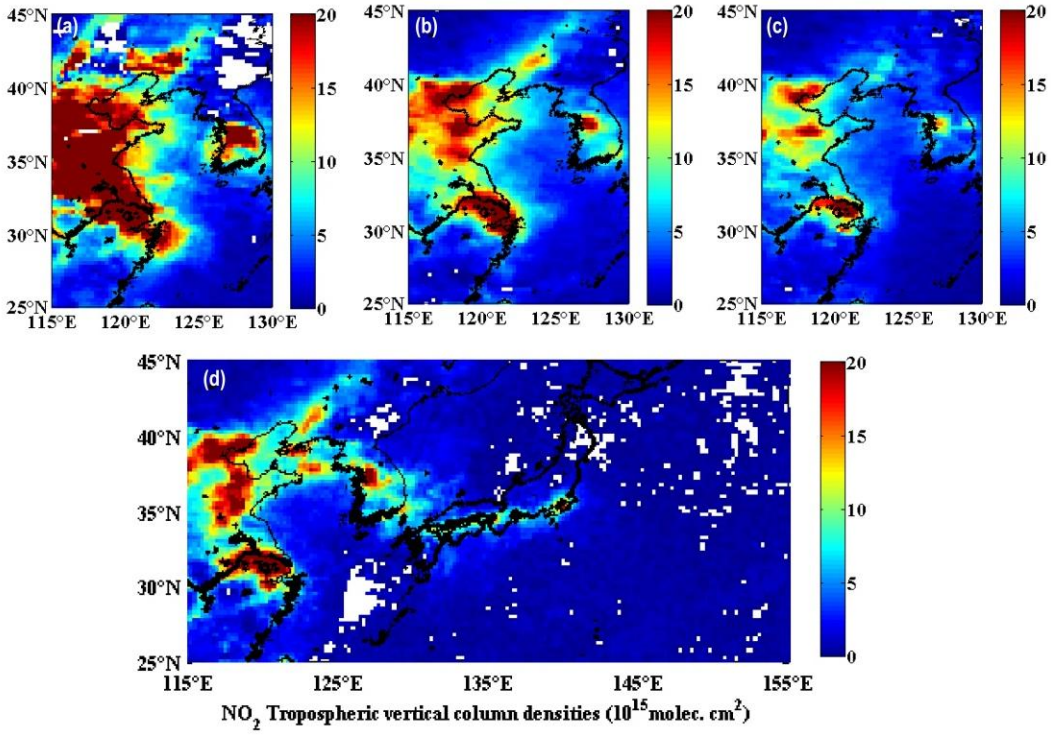

Figure S1 Satellite value of NO_2 (GOME-2 observation) during November 2012 (a), May 2014 (b), August 2015 (c) and April 2014 (d).

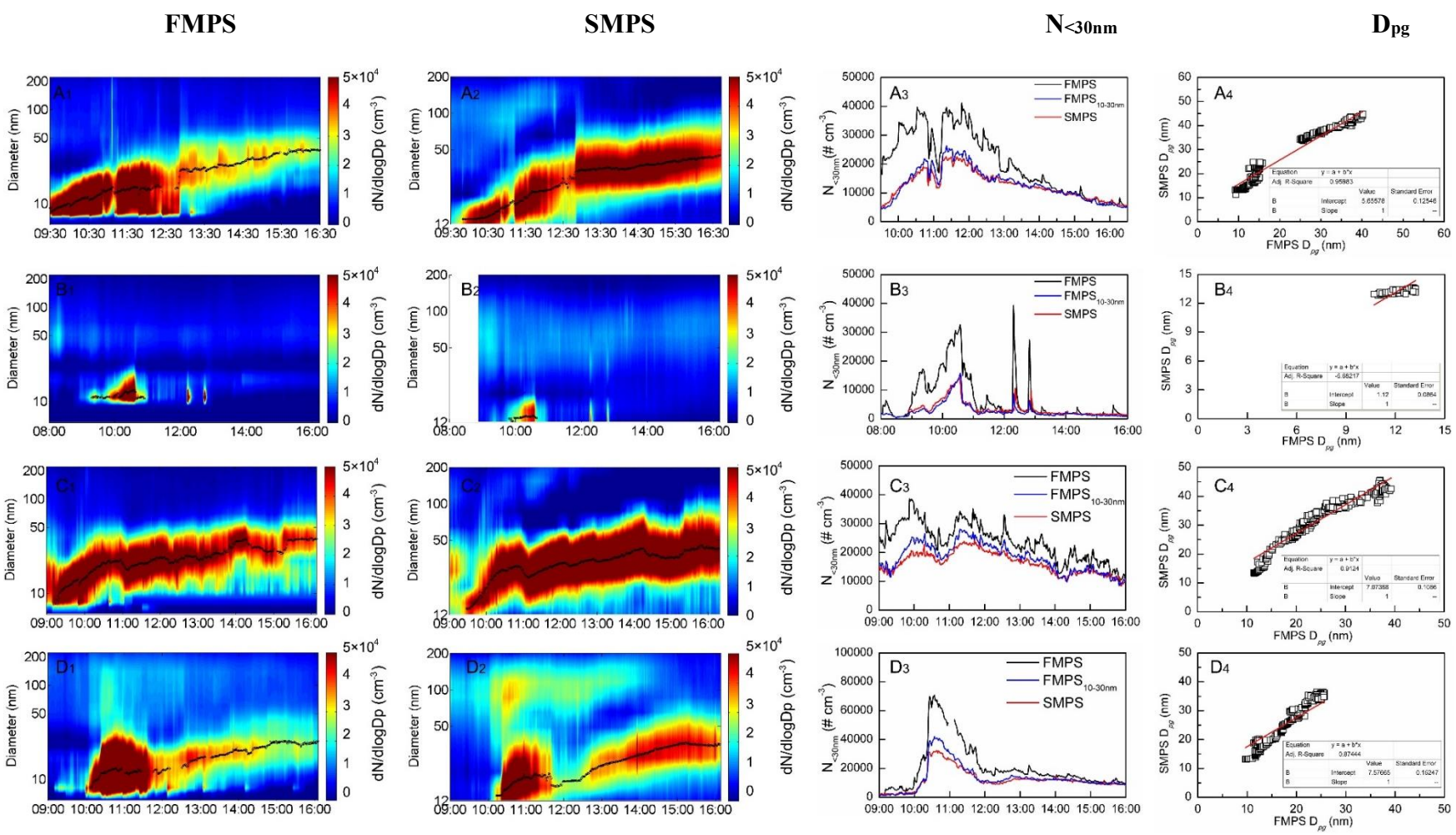

Figure S2 Comparison of $N_{<30\ nm}$ and D_{pg} during four NPF days in 2012 (A: 14 October, B: 15 October, C: 17 October, D: 18 October).

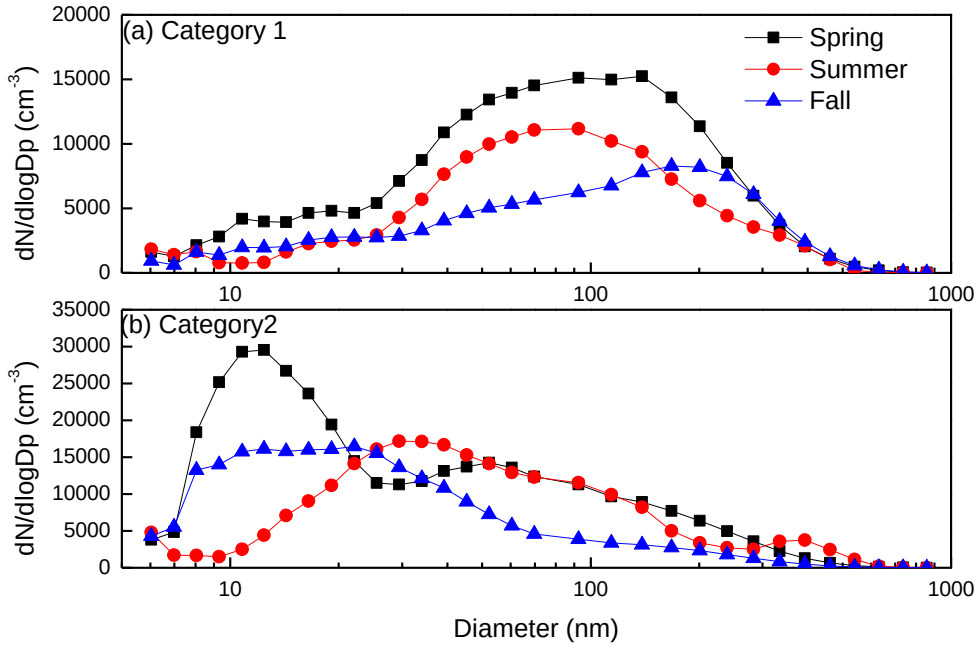

Figure S3 Seasonal variations in the average particle size distributions over the marginal seas of China.

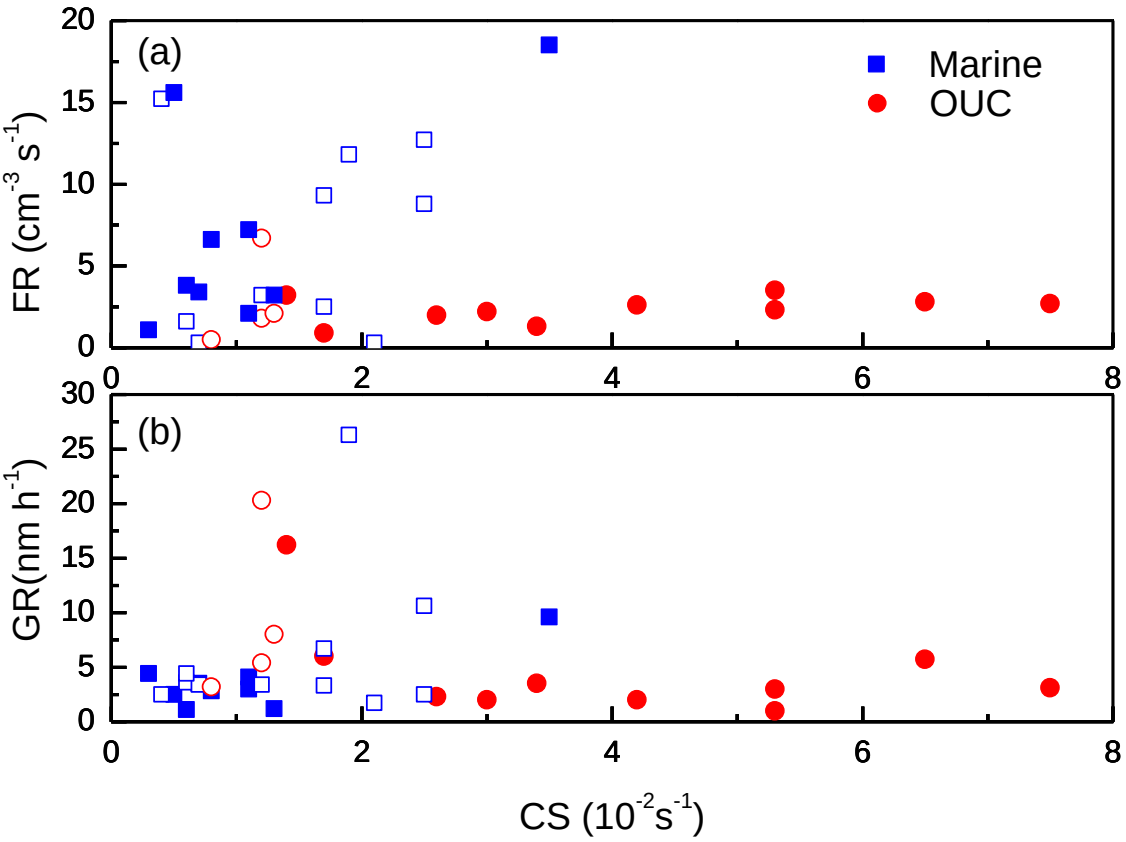

Figure S4 Relationship of the condensation sink (CS) with the formation rate (FR) and growth rate (GR) over the marine (NWPO and marginal seas) and at the OUC site (the solid markers represent the simultaneous NPF events).

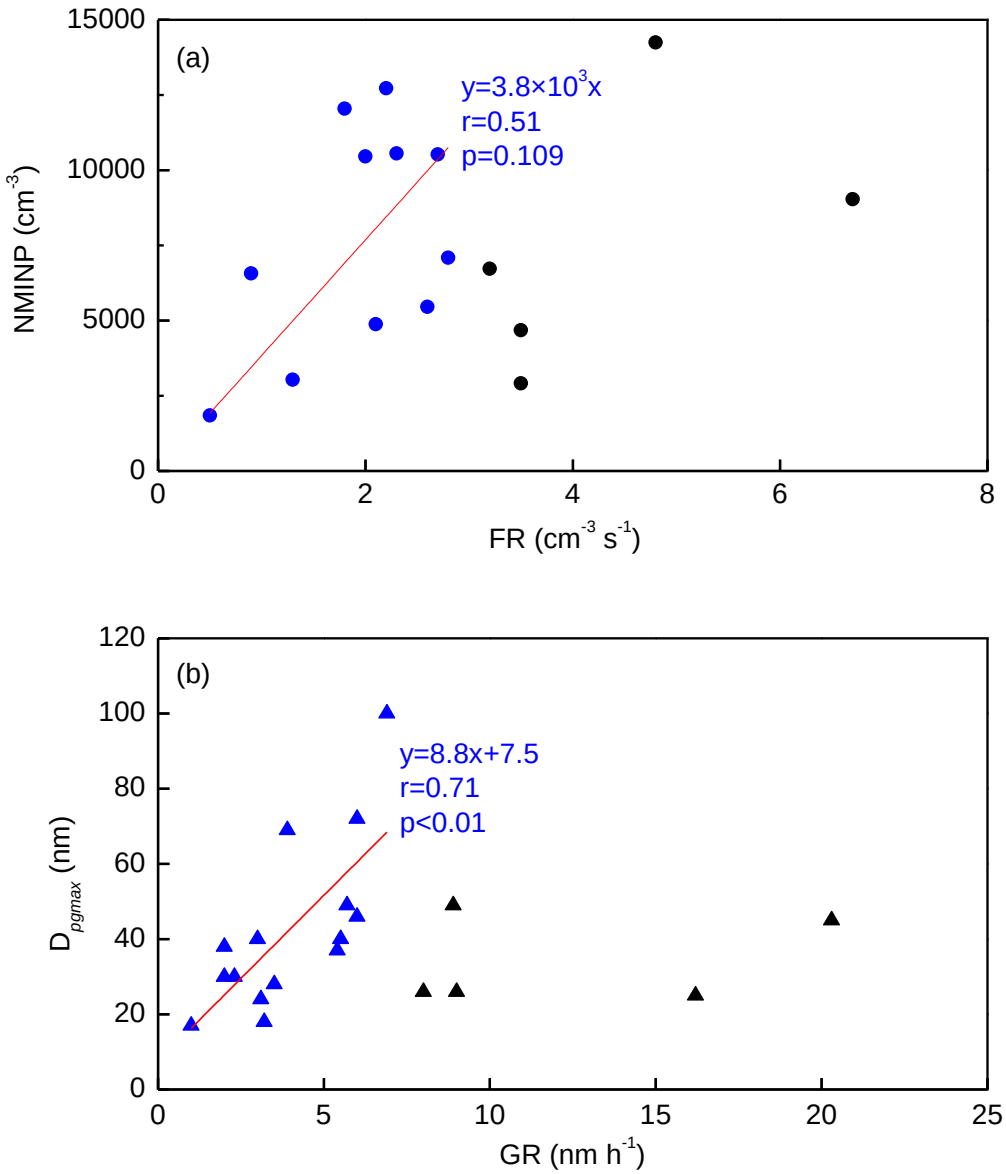

Figure S5 Relationship between the net maximum increase in the nucleation mode particles number concentration (NMINP) and new particle formation rate (FR), maximum geometric median diameter of new particles (D_{pgmax}) and growth rate (GR) in NPF events occurred at the OUC site (the black symbols were treated as outliers and excluded from the correlation analysis).

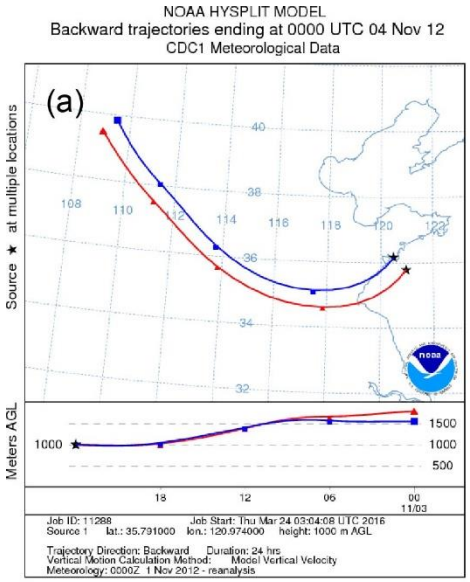
NOAA HYSPLIT MODEL
Backward trajectories ending at 0000 UTC 04 Nov 12
CDC1 Meteorological Data
(a)
Source ★ at multiple locations
Meters AGL
Job ID: 11288 Job Start: Thu Mar 24 03:04:08 UTC 2016
Source 1 lat.: 35.791000 lon.: 120.974000 height: 1000 m AGL
Trajectory Direction: Backward Duration: 24 hrs
Vertical Motion Calculation Method: Model Vertical Velocity
Meteorology: 0000Z 1 Nov 2012 - reanalysis

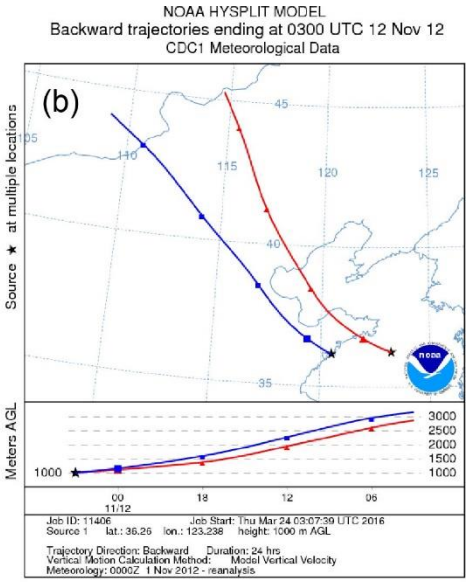
NOAA HYSPLIT MODEL
Backward trajectories ending at 0300 UTC 12 Nov 12
CDC1 Meteorological Data
(b)
Source ★ at multiple locations
Meters AGL
Job ID: 11406 Job Start: Thu Mar 24 03:07:39 UTC 2016
Source 1 lat.: 36.26 lon.: 123.238 height: 1000 m AGL
Trajectory Direction: Backward Duration: 24 hrs
Vertical Motion Calculation Method: Model Vertical Velocity
Meteorology: 0000Z 1 Nov 2012 - reanalysis

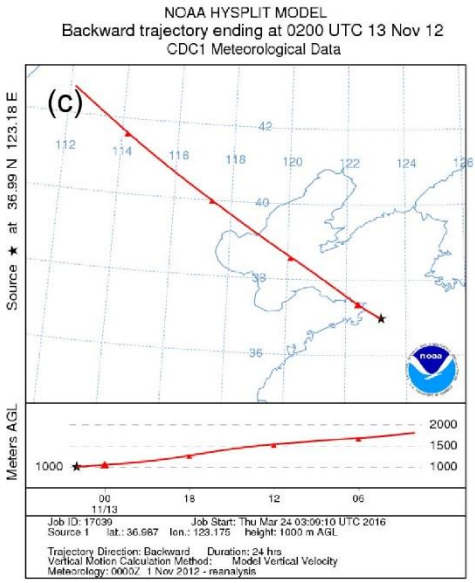
NOAA HYSPLIT MODEL
Backward trajectory ending at 0200 UTC 13 Nov 12
CDC1 Meteorological Data
(c)
Source ★ at 36.99 N 123.18 E
Meters AGL
Job ID: 17039 Job Start: Thu Mar 24 03:09:10 UTC 2016
Source 1 lat.: 36.987 lon.: 123.175 height: 1000 m AGL
Trajectory Direction: Backward Duration: 24 hrs
Vertical Motion Calculation Method: Model Vertical Velocity
Meteorology: 0000Z 1 Nov 2012 - reanalysis

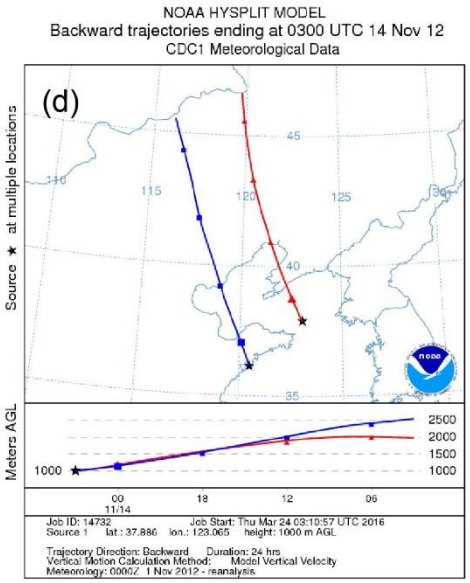
NOAA HYSPLIT MODEL
Backward trajectories ending at 0300 UTC 14 Nov 12
CDC1 Meteorological Data
(d)
Source ★ at multiple locations
Meters AGL
Job ID: 14732 Job Start: Thu Mar 24 03:10:57 UTC 2016
Source 1 lat.: 37.886 lon.: 123.065 height: 1000 m AGL
Trajectory Direction: Backward Duration: 24 hrs
Vertical Motion Calculation Method: Model Vertical Velocity
Meteorology: 0000Z 1 Nov 2012 - reanalysis

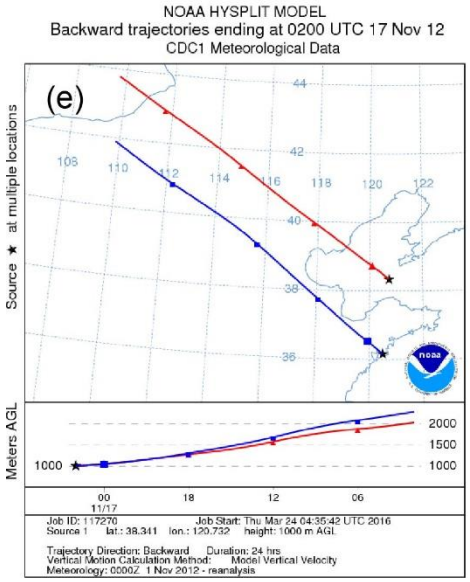
NOAA HYSPLIT MODEL
Backward trajectories ending at 0200 UTC 17 Nov 12
CDC1 Meteorological Data
(e)
Source ★ at multiple locations
Meters AGL
Job ID: 117270 Job Start: Thu Mar 24 04:35:42 UTC 2016
Source 1 lat.: 38.341 lon.: 120.732 height: 1000 m AGL
Trajectory Direction: Backward Duration: 24 hrs
Vertical Motion Calculation Method: Model Vertical Velocity
Meteorology: 0000Z 1 Nov 2012 - reanalysis

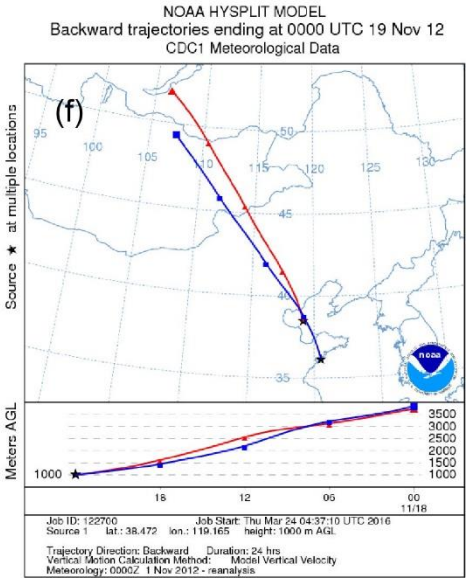
NOAA HYSPLIT MODEL
Backward trajectories ending at 0000 UTC 19 Nov 12
CDC1 Meteorological Data
(f)
Source ★ at multiple locations
Meters AGL
Job ID: 122700 Job Start: Thu Mar 24 04:37:10 UTC 2016
Source 1 lat.: 38.472 lon.: 119.165 height: 1000 m AGL
Trajectory Direction: Backward Duration: 24 hrs
Vertical Motion Calculation Method: Model Vertical Velocity
Meteorology: 0000Z 1 Nov 2012 - reanalysis

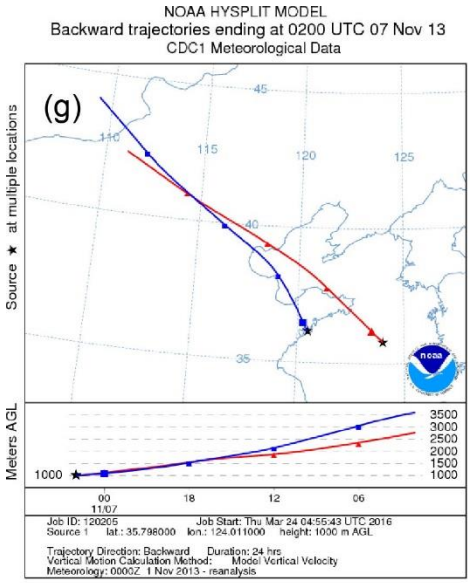
NOAA HYSPLIT MODEL
Backward trajectories ending at 0200 UTC 07 Nov 13
CDC1 Meteorological Data
(g)
Source ★ at multiple locations
Meters AGL
Job ID: 120205 Job Start: Thu Mar 24 04:55:43 UTC 2016
Source 1 lat.: 35.798000 lon.: 124.011000 height: 1000 m AGL
Trajectory Direction: Backward Duration: 24 hrs
Vertical Motion Calculation Method: Model Vertical Velocity
Meteorology: 0000Z 1 Nov 2013 - reanalysis

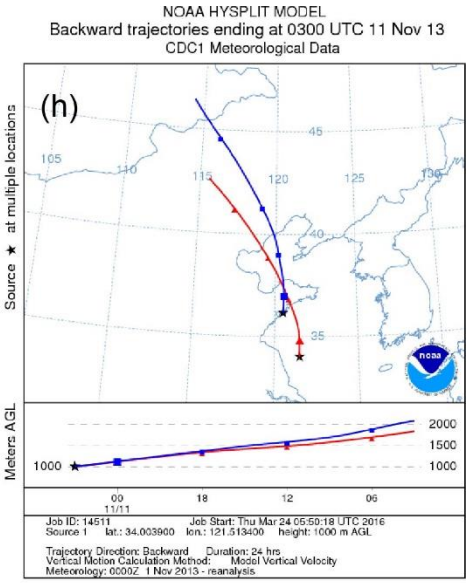
NOAA HYSPLIT MODEL
Backward trajectories ending at 0300 UTC 11 Nov 13
CDC1 Meteorological Data
(h)
Source ★ at multiple locations
Meters AGL
Job ID: 14511 Job Start: Thu Mar 24 05:50:18 UTC 2016
Source 1 lat.: 34.003900 lon.: 121.513400 height: 1000 m AGL
Trajectory Direction: Backward Duration: 24 hrs
Vertical Motion Calculation Method: Model Vertical Velocity
Meteorology: 0000Z 1 Nov 2013 - reanalysis

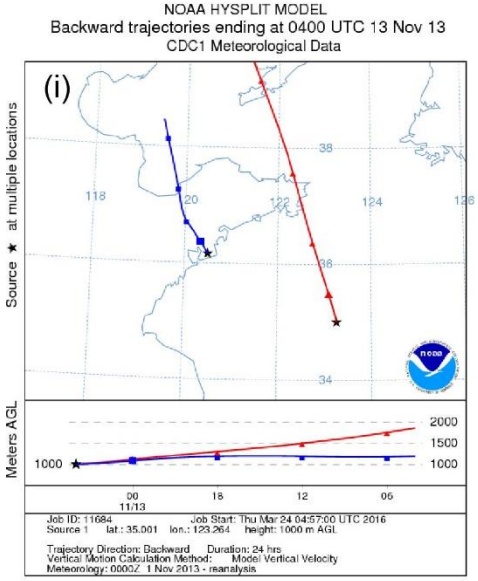
NOAA HYSPLIT MODEL
Backward trajectories ending at 0400 UTC 13 Nov 13
CDC1 Meteorological Data
(i)
Source ★ at multiple locations
Meters AGL
Job ID: 11684 Job Start: Thu Mar 24 04:57:00 UTC 2016
Source 1 lat.: 35.001 lon.: 123.264 height: 1000 m AGL
Trajectory Direction: Backward Duration: 24 hrs
Vertical Motion Calculation Method: Model Vertical Velocity
Meteorology: 0000Z 1 Nov 2013 - reanalysis

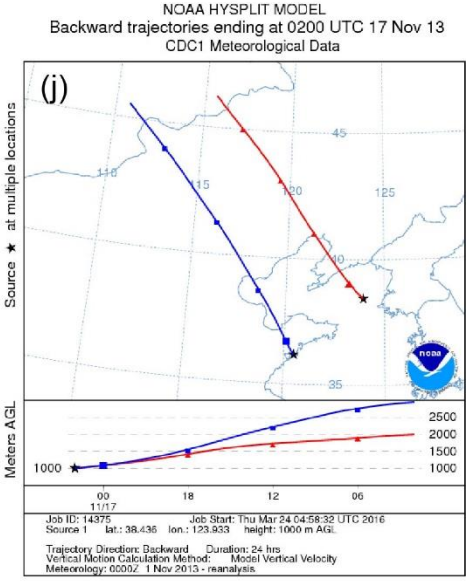
NOAA HYSPLIT MODEL
Backward trajectories ending at 0200 UTC 17 Nov 13
CDC1 Meteorological Data
(j)
Source ★ at multiple locations
Meters AGL
Job ID: 14375 Job Start: Thu Mar 24 04:58:32 UTC 2016
Source 1 lat.: 38.436 lon.: 123.933 height: 1000 m AGL
Trajectory Direction: Backward Duration: 24 hrs
Vertical Motion Calculation Method: Model Vertical Velocity
Meteorology: 0000Z 1 Nov 2013 - reanalysis

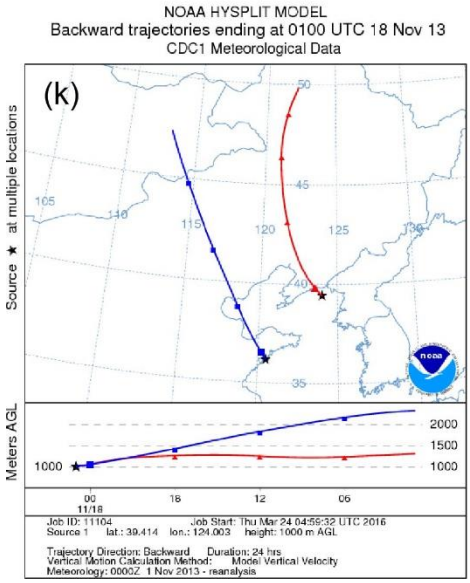
NOAA HYSPLIT MODEL
Backward trajectories ending at 0100 UTC 18 Nov 13
CDC1 Meteorological Data
(k)
Source ★ at multiple locations
Meters AGL
Job ID: 11104 Job Start: Thu Mar 24 04:59:32 UTC 2016
Source 1 lat.: 39.414 lon.: 124.003 height: 1000 m AGL
Trajectory Direction: Backward Duration: 24 hrs
Vertical Motion Calculation Method: Model Vertical Velocity
Meteorology: 0000Z 1 Nov 2013 - reanalysis

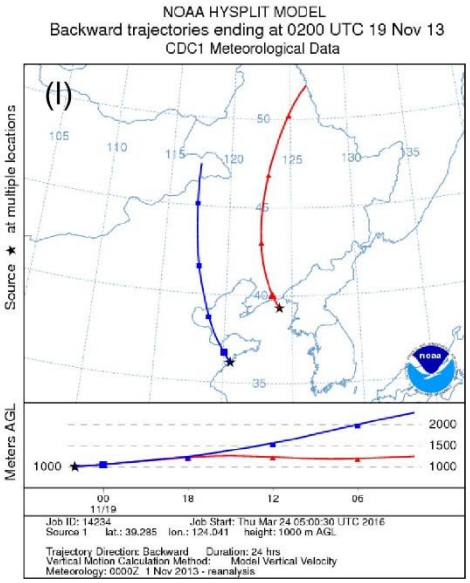
NOAA HYSPLIT MODEL
Backward trajectories ending at 0200 UTC 19 Nov 13
CDC1 Meteorological Data
(l)
Source ★ at multiple locations
Meters AGL
Job ID: 14234 Job Start: Thu Mar 24 05:00:30 UTC 2016
Source 1 lat.: 39.285 lon.: 124.041 height: 1000 m AGL
Trajectory Direction: Backward Duration: 24 hrs
Vertical Motion Calculation Method: Model Vertical Velocity
Meteorology: 0000Z 1 Nov 2013 - reanalysis

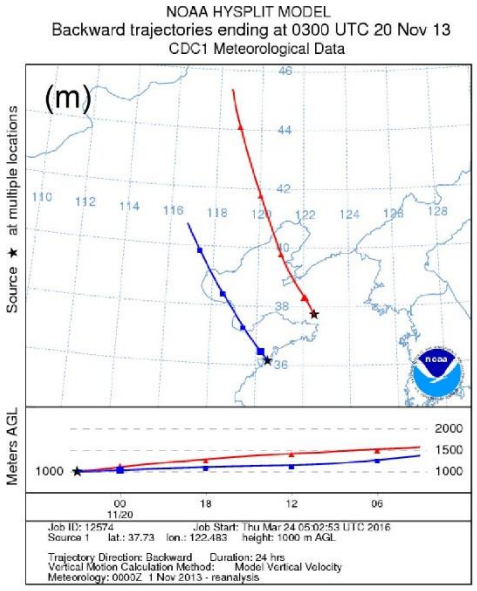
NOAA HYSPLIT MODEL
Backward trajectories ending at 0300 UTC 20 Nov 13
CDC1 Meteorological Data
(m)
Source ★ at multiple locations
Meters AGL
Job ID: 12574 Job Start: Thu Mar 24 05:02:53 UTC 2016
Source 1 lat.: 37.73 lon.: 122.483 height: 1000 m AGL
Trajectory Direction: Backward Duration: 24 hrs
Vertical Motion Calculation Method: Model Vertical Velocity
Meteorology: 0000Z 1 Nov 2013 - reanalysis

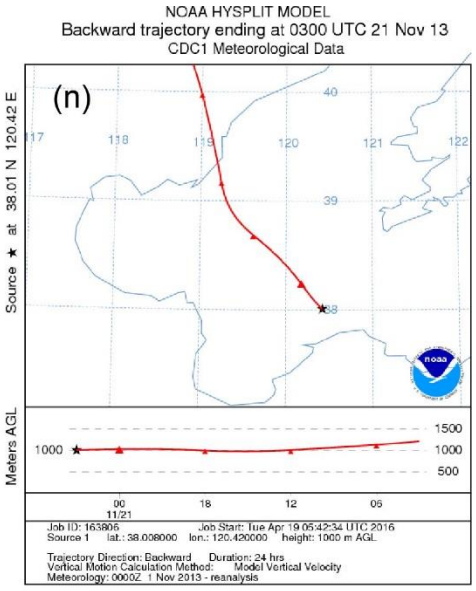
NOAA HYSPLIT MODEL
Backward trajectory ending at 0300 UTC 21 Nov 13
CDC1 Meteorological Data
(n)
Source ★ at 38.01 N 120.42 E
Meters AGL
Job ID: 163806 Job Start: Tue Apr 19 05:42:34 UTC 2016
Source 1 lat.: 38.008000 lon.: 120.420000 height: 1000 m AGL
Trajectory Direction: Backward Duration: 24 hrs
Vertical Motion Calculation Method: Model Vertical Velocity
Meteorology: 0000Z 1 Nov 2013 - reanalysis

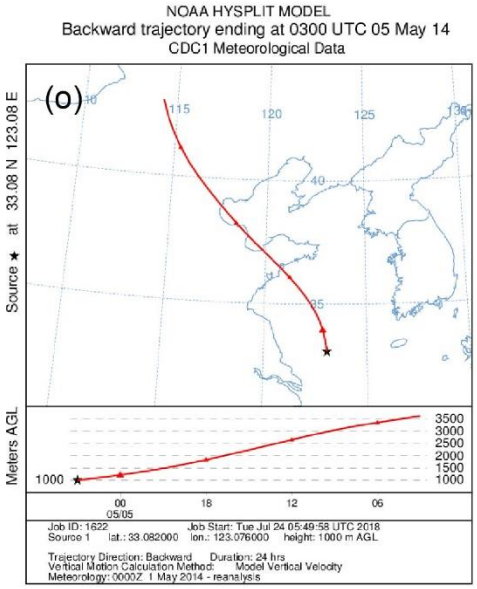
NOAA HYSPLIT MODEL
Backward trajectory ending at 0300 UTC 05 May 14
CDC1 Meteorological Data
(o)
Source ★ at 33.08 N 123.08 E
Meters AGL
Job ID: 1622 Job Start: Tue Jul 24 05:49:58 UTC 2018
Source 1 lat.: 33.082000 lon.: 123.076000 height: 1000 m AGL
Trajectory Direction: Backward Duration: 24 hrs
Vertical Motion Calculation Method: Model Vertical Velocity
Meteorology: 0000Z 1 May 2014 - reanalysis

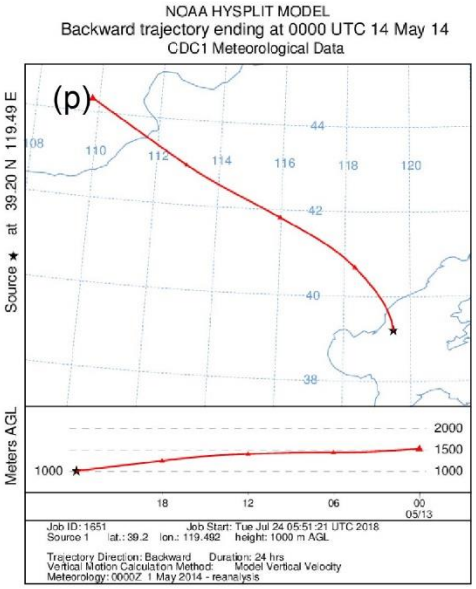
NOAA HYSPLIT MODEL
Backward trajectory ending at 0000 UTC 14 May 14
CDC1 Meteorological Data
(p)
Source ★ at 39.20 N 119.49 E
Meters AGL
Job ID: 1651 Job Start: Tue Jul 24 05:51:21 UTC 2018
Source 1 lat.: 39.2 lon.: 119.492 height: 1000 m AGL
Trajectory Direction: Backward Duration: 24 hrs
Vertical Motion Calculation Method: Model Vertical Velocity
Meteorology: 0000Z 1 May 2014 - reanalysis

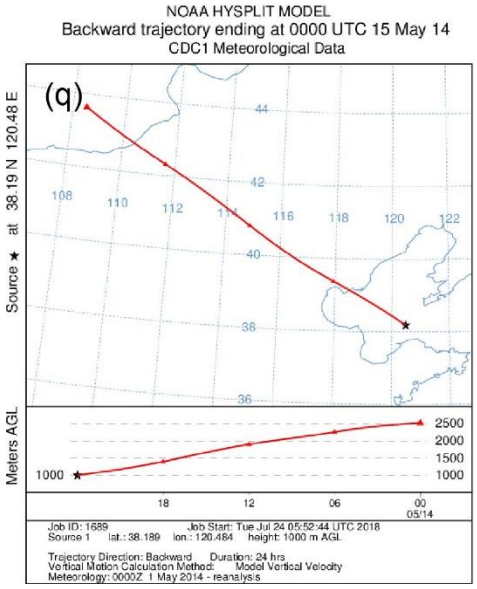
NOAA HYSPLIT MODEL
Backward trajectory ending at 0000 UTC 15 May 14
CDC1 Meteorological Data
(q)
Source ★ at 38.19 N 120.48 E
Meters AGL
Job ID: 1689 Job Start: Tue Jul 24 05:52:44 UTC 2018
Source 1 lat.: 38.189 lon.: 120.484 height: 1000 m AGL
Trajectory Direction: Backward Duration: 24 hrs
Vertical Motion Calculation Method: Model Vertical Velocity
Meteorology: 0000Z 1 May 2014 - reanalysis

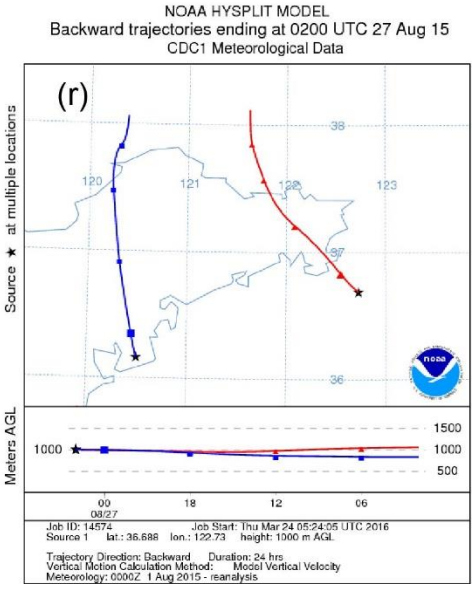
NOAA HYSPLIT MODEL
Backward trajectories ending at 0200 UTC 27 Aug 15
CDC1 Meteorological Data
(r)
Source ★ at multiple locations
Meters AGL
Job ID: 14574 Job Start: Thu Mar 24 05:24:05 UTC 2016
Source 1 lat.: 36.688 lon.: 122.73 height: 1000 m AGL
Trajectory Direction: Backward Duration: 24 hrs
Vertical Motion Calculation Method: Model Vertical Velocity
Meteorology: 0000Z 1 Aug 2015 - reanalysis

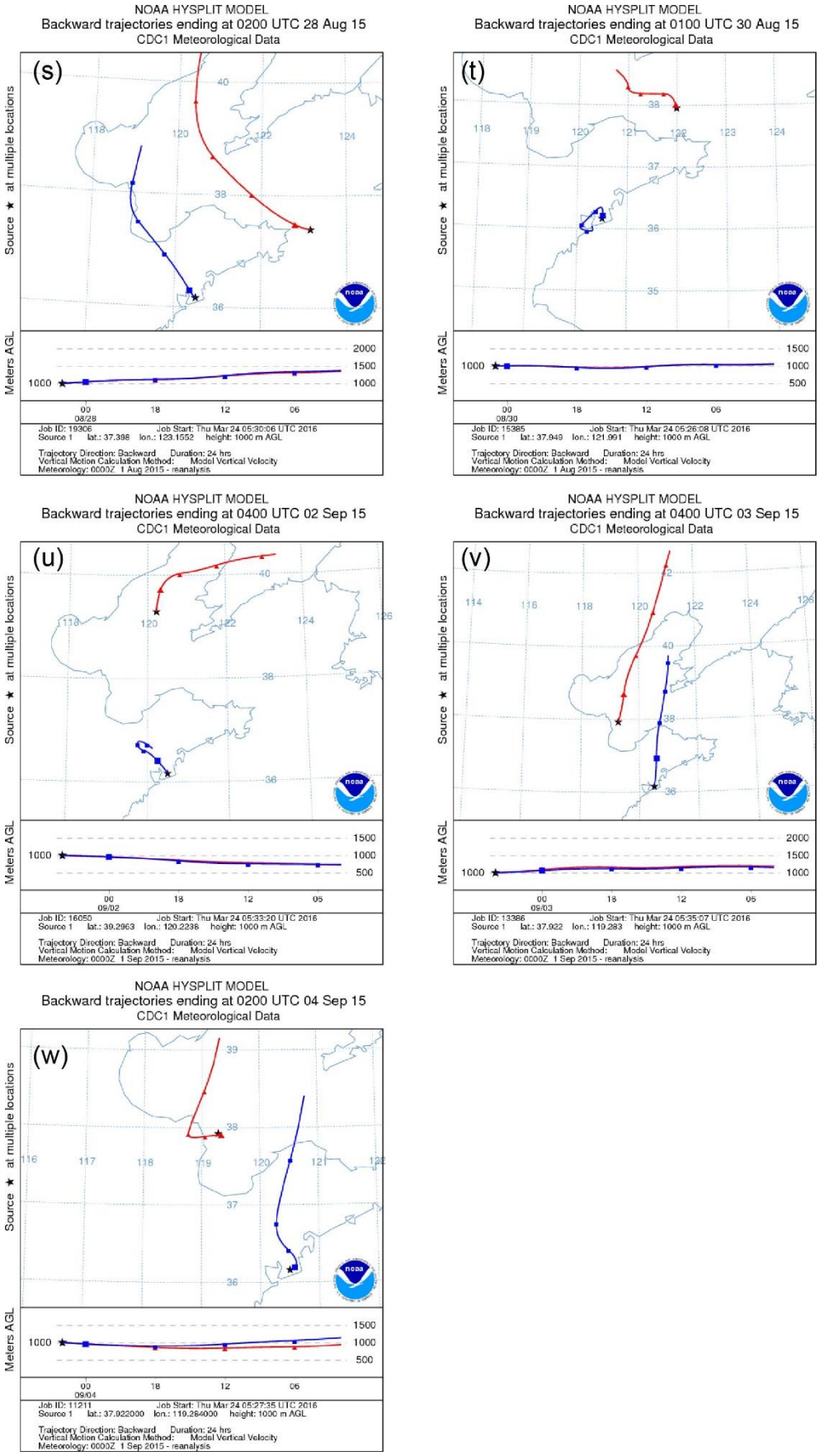

Figure S6 24-h air mass back trajectories on NPF days from 2012 to 2015 (the red lines represent the ship location, and the blue lines represent the location of OUC).

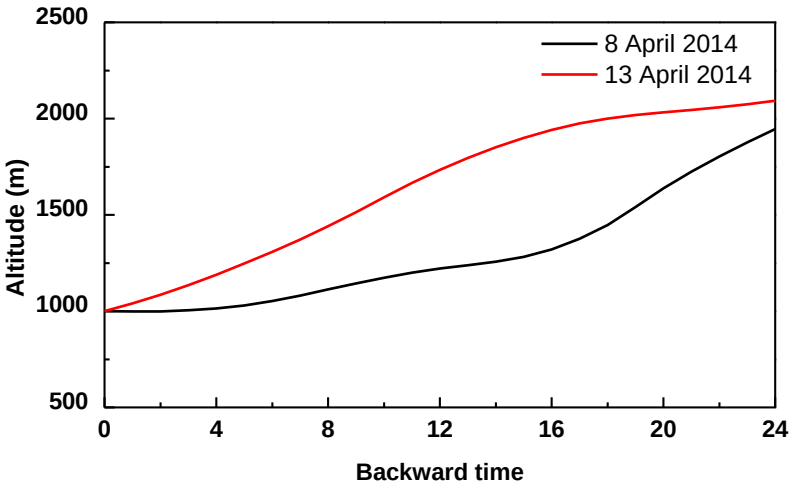

Figure S7 Height of the air mass back trajectories on 8 and 13 April 2014 over the NWPO.

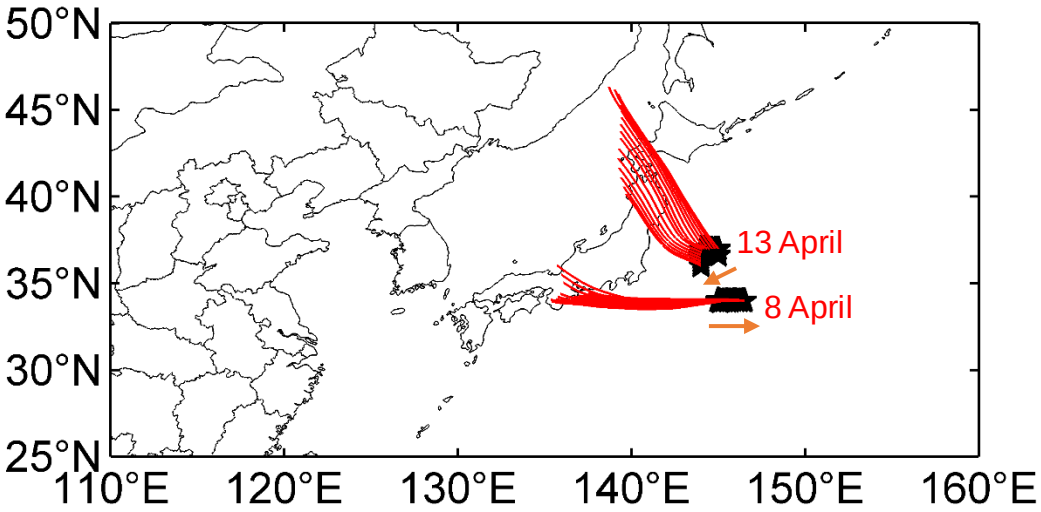

Figure S8 24-h air mass back trajectory throughout the NPF events and sampling periods (from 7:00 to 24:00 on 8 April 2014 and from 7:00 to 21:00 on 13 April 2014).

Table S1 Comparison of same NPF events measured by FMPS and SMPS.

		FR (particles cm^{-3})	GR (nm h^{-1})
14 October	FMPS	8.4	4.7
	$FMPS_{10\text{-}30nm}$	8.4	4.7
	SMPS	6.8	5
15 October	FMPS	7.3	
	$FMPS_{10\text{-}30nm}$	4.7	
	SMPS	4.2	
17 October	FMPS	6.8	3.7
	$FMPS_{10\text{-}30nm}$	6.8	3.7
	SMPS	6.2	4.5
18 October	FMPS	39.3	3.8
	$FMPS_{10\text{-}30nm}$	25.9	3.8
	SMPS	21.8	4.7